Heterogeneous & Homogeneous & Bio- & Nano-
CHEMCATCHEM
CATALYSIS

Accepted Article

Title: Layer-wise titania growth within dimeric organic functional group viologen periodic mesoporous organosilica as efficient photocatalyst for oxidative formic acid decomposition

Authors: Arefeh Ahadi, Hassan Alamgholiloo, Sadegh Rostamnia, Xiao Liu, Mohammadreza Shokouhimehr, Diego A. Alonso, and Rafael Luque

To be cited as: *ChemCatChem* 10.1002/cctc.201900486

Link to VoR: http://dx.doi.org/10.1002/cctc.201900486

A Journal of
ChemPubSoc Europe

WILEY-VCH www.chemcatchem.org

10.1002/cctc.201900486

Graphical Abstract

Layer-wise titania growth within dimeric organic functional group viologen periodic mesoporous organosilica as efficient photocatalyst for oxidative formic acid decomposition

Arefeh Ahadi, Hassan Alamgholiloo, Sadegh Rostamnia, Xiao Liu, Mohammadreza Shokouhimehr, Diego A. Alonso, Rafael Luque

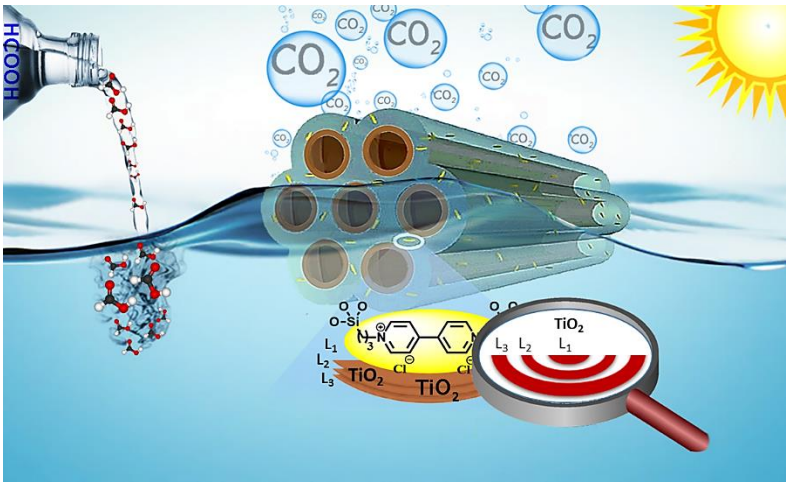

Layer-wise titania growth within dimeric organic functional group viologen periodic mesoporous organosilica as efficient photocatalyst for oxidative formic acid decomposition

Arefeh Ahadi, [a] Hassan Alamgholiloo, [a] Sadegh Rostamnia, *,[a] Xiao Liu, *,[b] Mohammadreza Shokouhimehr, *,[c] Diego A. Alonso, [d] Rafael Luque [e, f]

[a] *Organic and Nano Group (ONG), Department of Chemistry, Faculty of Science, University of Maragheh, PO Box 55181-83111, Maragheh, Iran. Tel:+98(421) 2276066; Fax: +98(421) 2276066; Email: rostamnia@maragheh.ac.ir; srostamnia@gmail.com*

[b] *Key Laboratory of Pesticide & Chemical Biology of the Ministry of Education, College of Chemistry, Central China Normal University, Wuhan 430079, P. R. China. Email: liuxiao71@tju.edu.cn*

[c] *Department of Materials Science and Engineering, Research Institute of Advanced Materials, Seoul National University, Seoul 08826, Republic of Korea. E-mail: mrsh2@snu.ac.kr*

[d] *Departamento de Química Orgánica and Instituto de Síntesis Orgánica (ISO), Facultad de Ciencias, Universidad de Alicante. Apdo. 99, E-03080 Alicante, Spain. Email: diego.alonso@ua.es*

[e] *Departamento de Quimica Organica, Universidad de Cordoba, Edificio Marie Curie, Ctra Nnal IV, Km 396, E-14014, Cordoba, Spain. Email: rafael.luque@uco.es*

[f] *Peoples Friendship University of Russia (RUDN University), 6 Miklukho Maklaya str., 117198, Moscow, Russia*

Abstract:

A bridge dimeric organic functional group viologen PMOs synthesized via layer by layer growth on titania (TiO_2) has been unprecedently prepared as stable periodic mesoporous organosilica using surfactant under mild acidic conditions. The layer by layer TiO_2 incorporation within the prepared organic functional group viologen-PMO could successfully develop a new type of hybrid photo-oxidation system for the mineralization of formic acid under sunlight irradiation conditions.

Keywords: Periodic mesoporous organosilica; viologen-based PMO; TiO_2; photo-oxidation; Formic acid.

1-Introduction

In recent years, photocatalytic formic acid degradation to CO_2 and H_2 has been studied widely [1-3]. Among the emerging photocatalysis technologies, those using sunlight as initial energy are the most competitive ones. For example, Yang's research team reported that the [001] facets of anatase TiO_2 (titania) show excellent photocatalytic activity due to their high surface energies and high percentage of [001] facets [4]. On the other hand, apart from efficiency, titania based catalytic systems for photo-oxidative formic acid (FA) processes are attractive due to their mechanism, photo-reaction pathway and CO_2 and H_2O production. However, there have been only a few studies successfully employing TiO_2 in photo-oxidation of FA and a few reports are in the catalytic strength of titania for this particular transformation [5-7]. Indeed, the design and synthesis of Ti-based photo-active catalyst for oxidation of FA is a crucial task towards this objective. Recently, Ide and co-workers investigated hydrothermal treatment of P25 to selectively convert the amorphous component into crystalline titania, which is deposited between the original anatase and rutile particles to increase the particle interfaces and thus enhanced charge separation for FA photo-oxidation [8].

FA has been recently considered as a potential liquid storage material capable of releasing H_2 under mild conditions via catalytic decomposition process [9,10]. The interest of this reaction has increased in the recent years because of the possibility of developing direct FA fuel cells (DFACs), that can reach high power densities and could be power sources for portable electronic devices [11,12]. On the other hand, FA is one of the major products of biomass processing that has been regarded as a convenient and safe hydrogen storage material because of its nontoxicity, high stability and high H_2 content (4.4 wt%).

Among the various forms of TiO_2, crystalline anatase has superior photo-activity properties. Several attempts have been made to incorporate titania into the porous silica framework such as

MCM-41, [13-15] MCM-48, [16,17] MSU, [18,19] mesocellar foam (MCFs), [20], SBA-15 [21-24], $mSiO_2$ [25] and organosilica [26] by simultaneous co-condensation of titanium and silicon precursors as titanosilicate scaffold or TiO_2/SiO_2 composite. The fabrication of such engineered titanosilicate composites generally leads to the dominant formation of the crystalline anatase titania [27,28]. In comparison, chemists have mostly ignored the basic advantages of amorphous TiO_2-based systems such as simple preparation process and relatively high surface area leading to high adsorptivity. In parallel with these studies, other investigations have developed on encapsulated amorphous titania for selective photocatalytic activity in organic reaction processes [26,29].

Periodic mesoporous organosilicas (PMOs) with an organic-inorganic hybrid framework have shown improved catalytic and photocatalytic properties in comparison to other materials [30]. These hybrid structures possess some obvious advantages over porous sol-gel derived or grafted hybrid materials such as highly ordered structures with very uniform pores, high loadings, and homogeneous distribution of functional groups throughout the whole framework [31,32]. However, despite the unique characteristic of PMOs, their impact as supports in photo-catalytic systems for environmental applications has been unexplored to date. Recently, our group has explored several PMO and PMO-type hybrid supports for encapsulation of transition metal nanoparticles and organic functional groups for catalytic aims [33-36]. We have also reported the synthesis and encapsulation of Pd nanoparticles for FA decompositions [33,35]. In this project, we present the synthesis and use of PMO with bridge organic functional group viologen as a dimeric skeleton and novel support for layer by layer growth of amorphous TiO_2. We also demonstrate the ability of this material in a selective photo-oxidation of FA under sunlight conditions.

2. Experimental

2.1. Materials and apparatus

(3-Chloropropyl)trimethoxysilane (CPTMS) was purchased from Fluka and 4,4′-bipyridine, Titanium (IV) butoxide and formic acid (FA) were obtained from Merck. The rest of the materials were also purchased from Sigma-Aldrich, Merck (Germany) and Fluka (Switzerland), and were used without further purification.

PMO materials were characterized by XRD measurements (Philips-PW 1800 diffractometer). Scanning electron microscopic (SEM) images were recorded on a Hitachi S-4800 filed emission scanning electron microscope (FE-SEM). Transmission electron microscopic (TEM) and elemental mapping images were taken by a JEM-2100F with an accelerating voltage of 200 kV. Fourier transform infrared (FT-IR) spectra were obtained using a Shimadazu IR-640 spectrometer, absorbancies are reported in cm^{-1}. Generated CO_2 in the reactor set-up was periodically and quantitatively analyzed by a gas chromatograph Thermal conductivity detector (TCD).

2.2. Preparation of Bipy-PMO

The mesoporous organosilica materials were synthesized based on our previous reports for the synthesis of PMOs [33-36]. Firstly, the synthesis of 4,4′-bipyridinium organic bridge was performed following previously reported methodology with certain modifications–[33-37]. Typically, 4,4'-bipyridine (0.5 g, 3.2 mmol) and 3-chloropropyltrimethoxysilane (2 mL, 10 mmol) were added to a two-necked 200 mL glass balloon in the presence of acetonitrile (10 mL). The reaction mixture was refluxed in the fully absence of light for 24 h. Then allowed to cool to room temperature. Thereafter, the solvent was removed by vacuum. The obtained viscous yellow ionic-liquid product was washed with pure *n*-hexane two times and then dried in vacuum, leading to the 4,4′-bipyridinium bridge with 96% yield. In a second step, in an Erlenmeyer flask containing 150 mL of a 2M HCl aqueous solution, 4 g of surfactant Pluronic P123 were stirred (overnight, 600 rpm) until dissolved. Then, the temperature reach to 35 °C. In a different flask, tetraethyl orthosilicate

(TEOS) and Bipy-IL linker (molar ratio of 4:1) were stirred in EtOH (5 mL) to obtain a clear yellow solution. Then, the yellow solution was dropwise added to the acidic surfactant solution and allowed to further stir during 4 h. Thereafter, the temperature of the mixture was increased to 40 ^{o}C and allowed to stir for 20 h. Then, the mixture was transferred to a stainless-steel autoclave and aged at 100 ^{o}C for 48 h. The surfactant was Soxhlet-extracted with EtOH during 100 h. Finally, the dimeric-based organic functional group viologen skeleton periodic mesoporous organosilica of Bipy-PMO/IL was obtained after drying under vacuum at 50 ^{o}C.

2.3. Synthesis of xTi_y@Bipy-PMO

For the synthesis of xTi_y@Bipy-PMO/IL (x=Ti% and y = number of cycles step for layer by layer TiO_2 growth), titanium (IV) butoxide [Ti(*n*-OBu)$_4$] was dropwise added to a toluene (25 mL) solution of Bipy-PMO. In a nitrogen atmosphere for the growth of the first layer of titania, Bipy-PMO/IL (1 g) was added to an anhydrous toluene (10 mL) solution of Ti(*n*-OBu)$_4$ (340 μL) at 110 °C. The reaction was stirred at this temperature for an additional 1 h. The obtained solids were successively washed with toluene and ethanol. Then, the Ti_1@Bipy-PMO was dried at 60 °C for 2 h. The formula of synthesized TiO_2@Bipy-PMO was described as 1.2Ti_1@Bipy-PMO based on the elemental analysis results. For the preparation of the material with a higher Ti loading (Ti_y@Bipy-PMO, y = 2-4), the above described methodology was iteratively carried out. Thus, various TiO_2@Bipy-PMO were synthesized and described as 1.2Ti_1@Bipy-PMO, 2.0Ti_2@Bipy-PMO, 2.7Ti_3@Bipy-PMO (with band gap 3.3 eV) and 3.3Ti_4@Bipy-PMO based on the elemental analysis results.

2.4. Typical procedure for photo-oxidation of FA

In a typical method, formic acid (5% vol, 5 mL-saturated with molecular O_2) was added to a stainless-steel container (75 mL) equipped with a Pyrex glass window together with 5 mg (**Figure 4c**) of 2.7Ti_3@Bipy-PMO catalyst. Then, the headspace of container was evacuated with Ar and sealed tightly. Then, the suspension was irradiated by full-spectrum simulated solar light ($\lambda > 300$ nm, 1 Sun (1000 Wm^{-2}) power), allowing band gap (UV light) excitation of the TiO_2. The reaction progress was monitored by collecting a definite amount of headspace gas with a syringe and further analysis by gas chromatography for 0, 30, 60 and 90 min (**Figure 4b**). The reaction temperature was not maintained during the irradiation process (increased ~5 ^oC for 90 min).

3. Results and discussion

In the present study, we used bipyridinium chloride dimeric-based PMO framework to our layer by layer growth of titanium dioxide. In fact, we demonstrate a facial preparation method for the synthesis of 3D mesoporous organosilica loaded with amorphous TiO_2 (xTi_y@Bipy-PMO) on both external and internal channels of the mesopores. On the other hand, by embedding the Dimeric organic functionality within the pore walls, the hydrophobic-hydrophilic properties of the PMO is well controlled. A schematic illustration of the xTi_y@Bipy-PMO synthesis is shown in Figure 1. Also, the bridging ligand and pores structure of PMO plays a vital role on the good control of the TiO_2 size and its homogeneous dispersion, thus enhancing the catalytic activity for the photo-oxidation of FA.

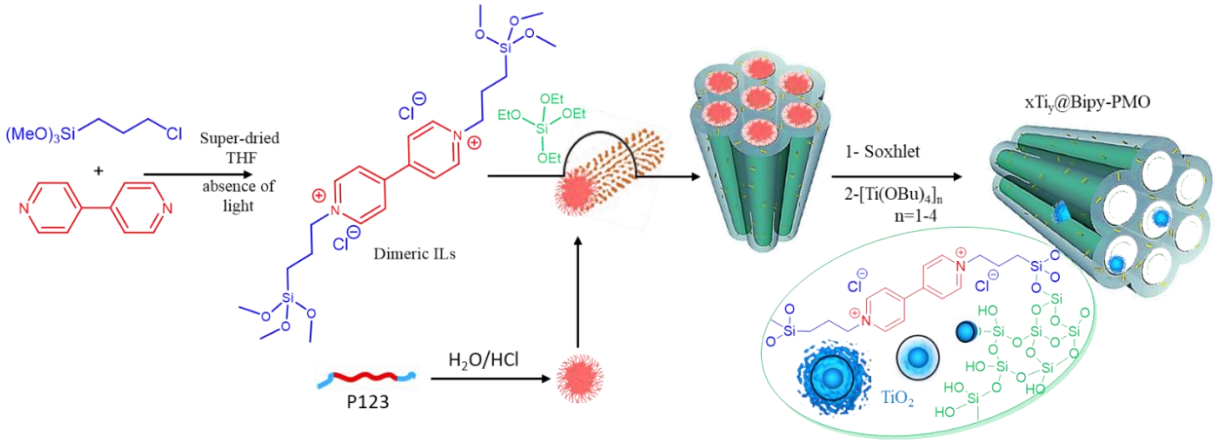

Figure 1. Schematic synthesis xTi_y@Bipy-PMO and layer by layer TiO_2-loading.

The obtained Ti@Bipy-PMO samples were characterized using several techniques including Powder X-ray Diffraction (PXRD), Brunauer-Emmett-Teller (BET), Scanning Electron Microscopy (SEM), SEM-EDX, Transmission Electron Microscopy (TEM), SEM-mapping, Atomic Absorption Spectroscopy (AAS) and Thermal Gravimetric Analysis (TGA and DTG). The low angle X-ray diffraction is used to study the porosity on the organosilica structure of Bipy-PMO. As shown in **Figure 2a**, a narrow peak appeared at $2\theta = 0.85$ (d = 10.9 nm) which is attributed to the presence of mesopores with uniform pore size in the PMO-Bipy structures. After the titania growth into pore of PMO, the X-ray diffraction low angle for $2.7Ti_3$@Bipy-PMO (selected as best catalysis for FA oxidation) was similar to that of Bipy-PMO [38]. However, PXRD indicated the absence of any crystalline TiO_2 domains (**Figure 2a**, inset). On the other hand, N_2 adsorption-desorption isotherms for Bipy-PMO, $1.2Ti_1$@Bipy-PMO and $2.7Ti_3$@Bipy-PMO, as shown in **Figure 2c**, showed a type IV curve with a hysteresis loop in the relative pressure of 0.45-1.0, which demonstrated the mesoporous structure. As represented in **Figure 2c,** titanium oxide layer by layer growth into the pore cage of PMO-Bipy is evidenced with a simultaneous decrease of the mesoporous surface areas from 473 cm^2/g for PMO-Bipy to 265 cm^2/g for $2.7Ti_3$@ PMO-Bipy. As calculated from the Barrett-Joyner-Halenda (BJH) method, the average

pore size for PMO-Bipy and Ti_3@PMO-Bipy were 3.3 and 2.1 nm, respectively. To estimate the ratio of organic moiety to silica in PMO structure of PMO-Bipy, thermogravimetric analysis (TGA), Derivative thermogravimetry (DTG), Differential Thermal Analysis (DTA) were achieved **Figure 2b**. Based on the TG analysis, a 400 μg weight loss was observed between 100 and 500 ^oC which might be attributed to the decomposition of the organic moieties of the PMO-Bipy (initial weight 5.57 mg).

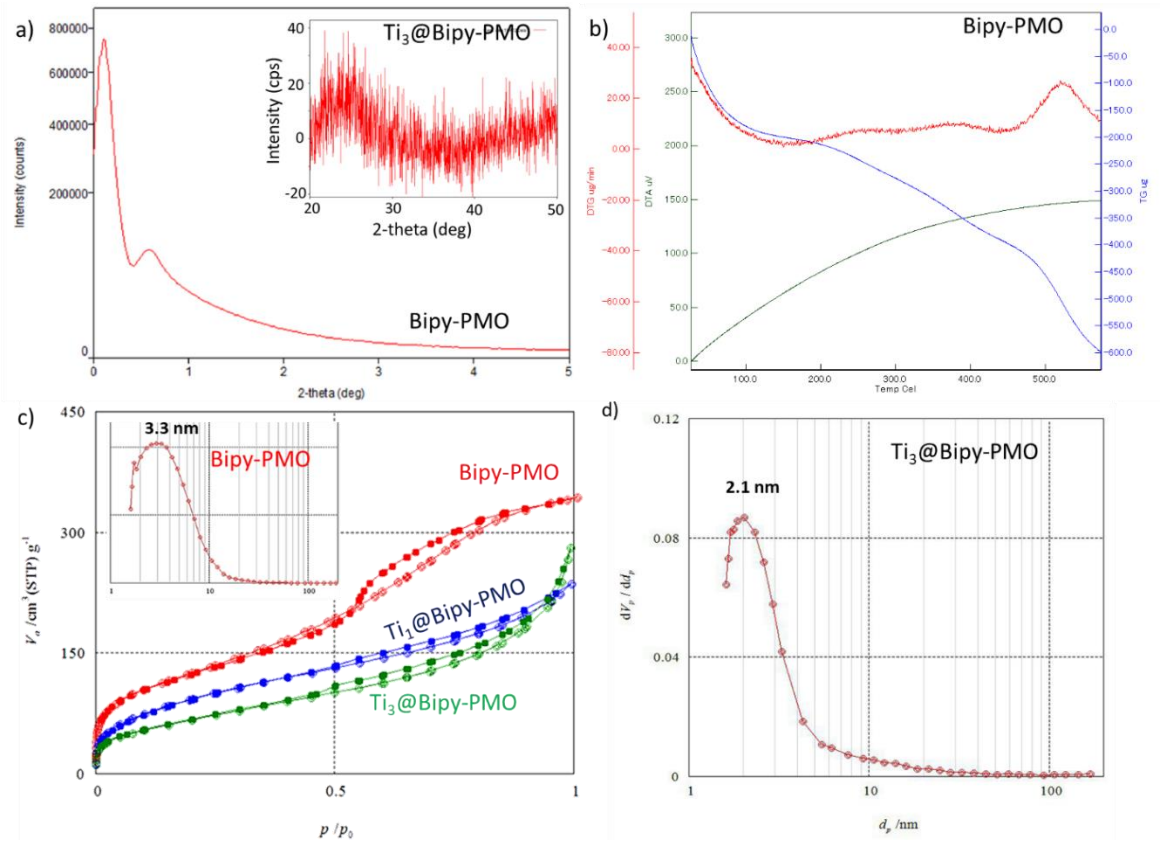

Figure 2. (a) low angle X-ray scattering of PMO-Bipy and inset diagram (Ti_3@Bipy-PMO), (b) TG-DTG-DTA profiles of Bipy-PMO (c and d) N_2 adsorption-desorption profile and BJH-Plot of Bipy-PMO and Ti_3@Bipy-PMO.

The morphology of the obtained PMO has been investigated through FE-SEM, TEM, while the elemental composition was studied by EDS and HAADF-STEM mapping as shown in **Figure 3**. FE-SEM images exhibited a sponge-like morphology of the Bipy-PMO and even four time TiO_2

growth (**Figures 3a,b** see also ESI). However, after the 4th layer titania growth, the PMO morphology barely shows the TiO_2 particles outside of PMO pores (**Figures 3c** and SI). TEM analysis of Bipy-PMO and Ti@Bipy-PMO clearly demonstrated the porous nature of the material with titania inside. The sponge-like porous structures were precisely investigated using TEM analysis (**Figure 3d, e, f**). As shown in **Figure 3d**, the as-synthesized PMO of Bipy-PMO structure possesses a 3D mesoporous structure. According to TEM images of Ti_1@Bipy-PMO (**Figure 3e**) and Ti_3@Bipy-PMO (**Figure 3f**), the mesoporous structure can be clearly identified for all samples in which TiO_2 particles are encapsulated.

High Angle Annular Dark Field STEM (HAADF-STEM) mapping results **(Figure 3g**) showed that each element (Si, N, O, C and Ti) is well dispersed on the Ti_3@Bipy-PMO structure. It is observed from (**Figure 3h**) that titania are distributed uniformly in the channel of the Bipy-PMO. The collected data from energy dispersive X-ray (EDX) analysis of the Ti_3@Bipy-PMO is shown in (**Figure 3i**). Based on this analysis, silicon, carbon, oxygen and titanium atoms exist in the structure, which indicates the high purity and perfect TiO_2 layer by layer growth into pore PMO support (for more information, see SI).

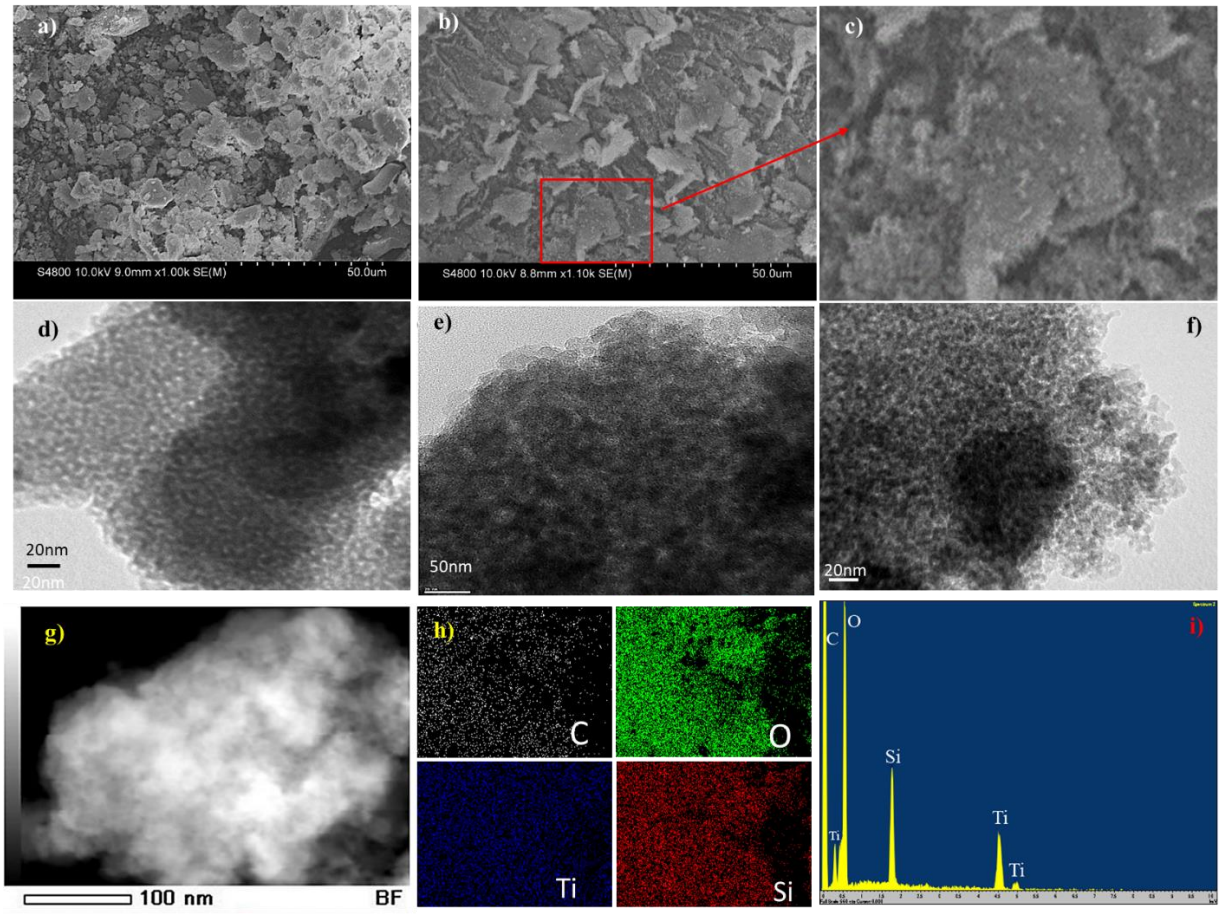

Figure 3. FE-SEM and TEM images of Bipy-PMO (a,d). FE-SEM and its zoomed SEM of Ti_3@Bipy-PMO and Ti_4@Bipy-PMO (b,c). TEM images of Bipy-PMO (d), Ti_1@Bipy-PMO and Ti_3@Bipy-PMO (e,f). HAADF-STEM image (g) and elemental maps of C, O, Si and Ti, extracted from the STEM image (h) and EDS analysis (i) of Ti_3@Bipy-PMO.

Finally, after the characterization of Ti@Bipy-PMO, this material was tested in the photo-oxidation of FA using sunlight simulator irradiation. Oxygen saturated FA photo-oxidation produces CO_2 and H_2O, without formation of intermediate products or multiple reactions [5-7]. To evaluate the performance of Ti@Bipy-PMO mesoporous for the photo-oxidation reaction, we utilize HCOOH as the reaction substrate. Whereas FA does not decompose at 300-350 K on pure TiO_2 [39], treatment FA with solar simulator in presence our Ti-PMO induced the occurrence of the reaction.

FA photo-oxidation reaction was then carried out by placing the series of Ti-PMO in 5 mL of FA (5% vol) at room temperature. We found that solvent, temperature, reaction time and loading of encapsulated titania into the PMO have a critical effect on the progress of the photo-oxidation process. Using these catalysts, CO generation was negligible while CO_2 generation was well-correlated with *literature* data[39]. The photocatalytic activities of our materials were strongly depended on the TiO_2 layer by layer growth **(Figure 4a**). The results clearly demonstrated an increase of the photocatalytic activity after the titania layer by layer growth into porous Bipy-PMO.

In this work, we firstly studied the reaction progress by varying the xTi_y@Bipy-PMO (y = 0-4) catalysts at 25 ºC. The results showed that all of the Ti-based PMOs are active for FA photo-oxidative process. Also, under similar conditions (for example, 5 mg of Ti_3@Bipy-PMO containing 0.0028 mmol encapsulated amorphous TiO_2) the activity depends on layers' growth of TiO_2. For Ti_3@Bipy-PMO and Ti_4@Bipy-PMO, the amount of CO_2 has a tangible variation. However, as can be observed in the SEM images, after Ti_3@Bipy-PMO addition of more titania source wrest the generation of non-encapsulated excess titania out of PMO channels as separated particle (**Figure 3b, c**).

Even though Ti_4@Bipy-PMO composite generated the highest amount of CO_2, we continued our reaction conditions optimization with encapsulated Ti_3@Bipy-PMO. Regarding the solvent effect, we studied the photo-oxidation progress with different solvents including, MeOH, EtOH, DMF, MeCN, and H_2O, showing the latest the highest turnover frequency (TOF) 187.82 (**Figure 4a)**. On the other hand, when the reaction was examined at various temperatures (H_2O as solvent), it was observed an increase of the reaction rate with the temperature. Despite this temperature effect on the yield, we continued our studies at room temperature due to energy issues. By using this study, kinetic parameters were also obtained (**Figure 4b**, inset). According to Arrhenius equation, the

activation energy from experimental results was 60.03 kJ.mol^{-1}. By increasing the amount of the catalyst from 5 mg to 20 mg, the FA oxidation was also increased (**Figure 4c**).

Photo-oxidation performance and synergistic effect of loading titania in the framework structure of PMO were studied based on the amount of generated gases, TONs and TOFs during the reaction **(Figure 4d)**. The photo-oxidation was strongly depended on the TiO_2 layer by layer growth, as represented in **Figure 4d** (inset), for the photo-oxidation activity with Ti_1@ PMO-Bipy (TON: 196.46) and Ti_4@ PMO-Bipy (TON: 340.21). The optimum activity was observed for Ti_4@ PMO-Bipy (TOF 252.78 h^{-1}; TON 340.21) due to a larger titania (not aggregated) loaded within PMO.

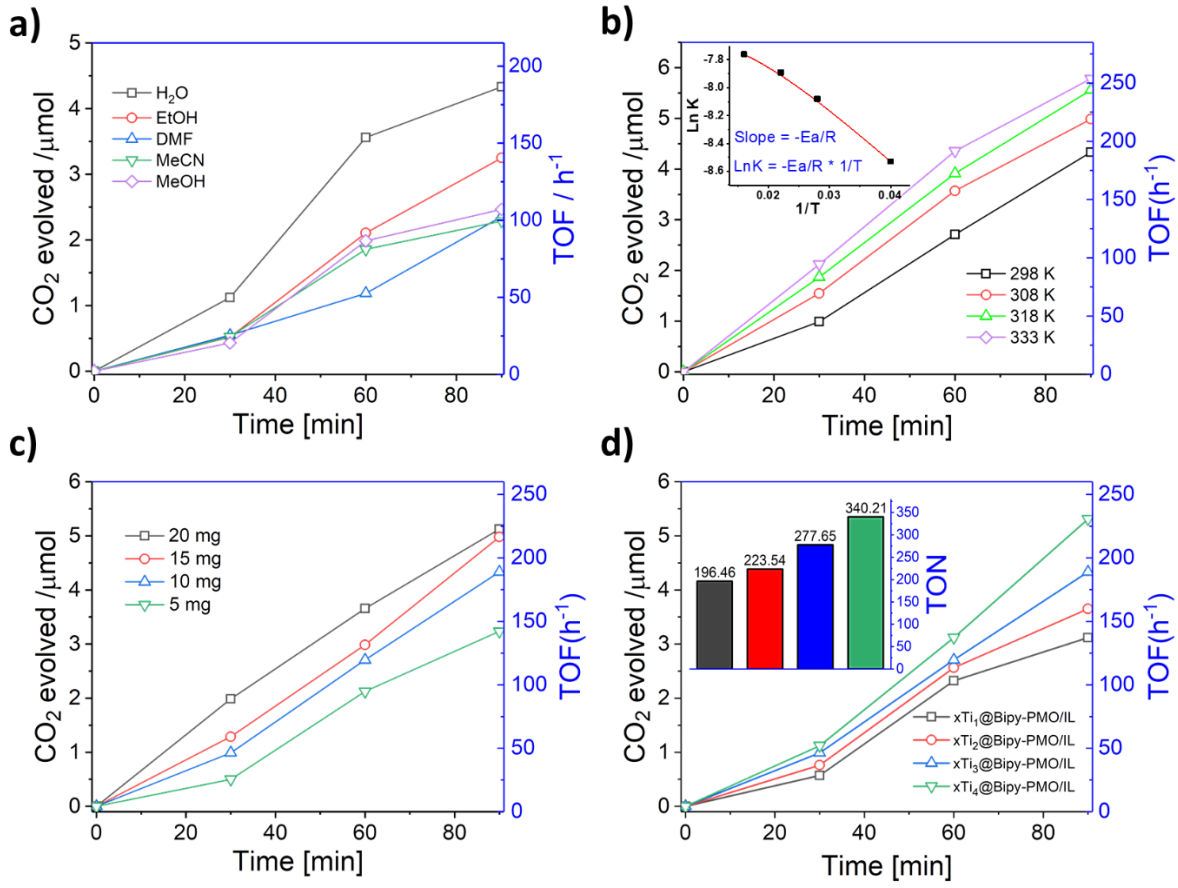

Figure 4. a) Study of the solvent effect under the similar conditions by the catalysis of xTi_3@Bipy-PMO at room temperature, b) Study of the reaction progress at different temperatures under the similar

conditions, c) Effect of catalyst amount to the same batch of the reaction at ambient condition in solution of FA (5 v/v%); d) Time courses of CO_2 evolution from FA (5 v/v%) on xTi_1@Bipy-PMO to xTi_4@ Bipy-PMO.

Finally, the reusability of Ti-PMO was tested by performing repeated reaction cycle using of Ti_3@Bipy-PMO under the optimized reaction condition. The catalyst after each reaction cycle was recovered by centrifugation and reactivated by washing it with ethanol (30 mL) for several times and then dried in an oven/vacuum. Finally, before re-using the catalyst, it was vacuumed at 120 ºC for 3 h. As shown in **Figure 5a,** a small decrease of yield was observed with after each reaction cycle which could be ascribed to the fact that a small fraction of the catalyst is lost in each recovery [38]. TEM image testified the stable structure of the solid catalyst after the reuse **Figure 5b**.

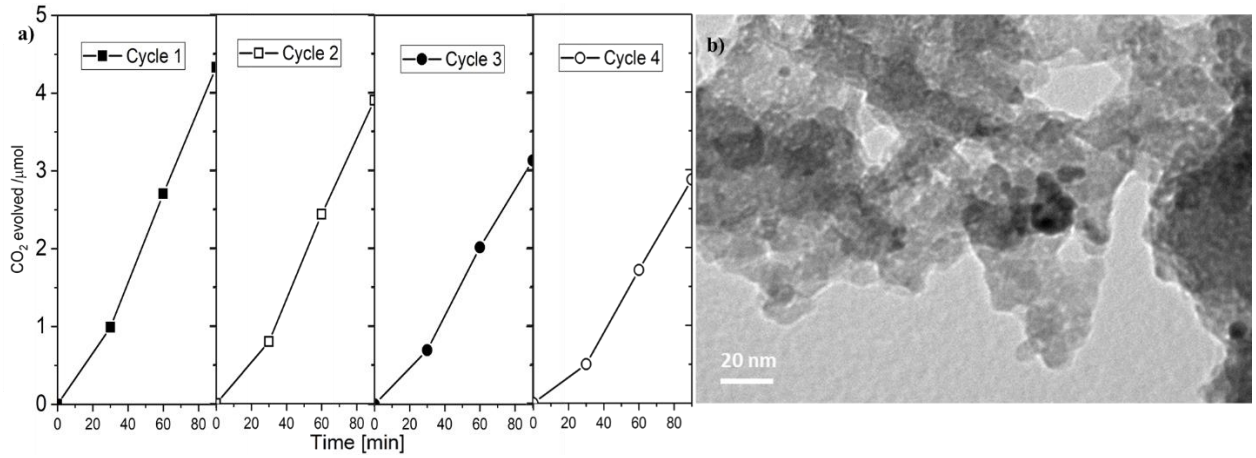

Figure 5. a) Reusability of the catalyst in four consecutive runs, b) TEM images after the 4th recycling of Ti_3@Bipy-PMO.

Dissolved/adsorbed oxygen ($O_{2\,(ads)}$) plays an important role in the photo-oxidation of FA [40,41]. On the other hand, studies of FA reaction on TiO_2 metal oxide encapsulated viologen-based PMO (PMO-V^{2+}) revealed that HCOOH can dissociatively adsorb on surfaces resulting in adsorbed

formate [$HCOO^-_{(ads)}$]. The scheme of HCOOH conversion to carbon dioxide is proposed as shown in the following equations [7,40]. The decomposition of FA process can therefore be described by the following sequence of photo-oxidation process (Scheme 1). Dicationic viologen parts of PMO can also act as an electron mediator between e/h to enhance photocatalyst life-time and avoid the recombination of those and photo-initiator of O_2^- generation in the presence of oxygen [42, 43].

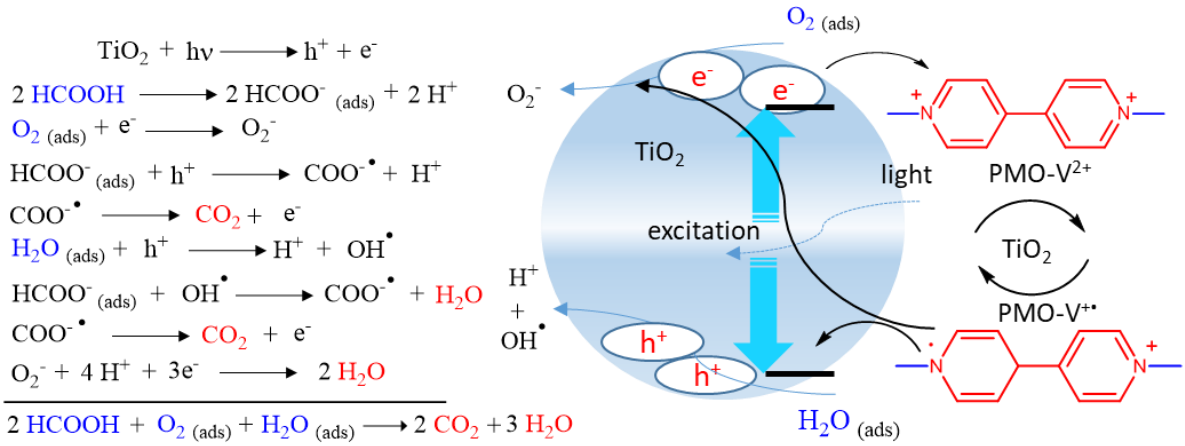

Scheme 1: Sequence of photo-oxidation process of FA [(ads) = adsorbed on TiO_2 surface].

4. Conclusions

In summary, we were able to successfully prepare, a relatively dimeric-based organic functional group viologen skeleton periodic mesoporous organosilica via co-assembly of as-synthesized bipyridinium linker and TEOS in the presence of structure directing agent of P123. Then, photo-oxidation of formic acid was separately addressed *via* incorporation of layer by layer growth amorphous titania inside of the Bipy-PMO support under sunlight irradiation. Kinetic studies showed that the TiO_2@PMO catalyst is active enough to catalyze the reaction in high efficiency. The TiO_2@PMO catalyst can also be easily recycled and reused at least four cycles without apparent loss of activity and production of carbon monoxide.

Conflicts of interest

There are no conflicts to declare.

Acknowledgements

The authors are thankful for financial supports (95849156) from Iran National foundation of Science (INSF). The publication has been prepared with support from RUDN University Program 5-100.

References

(1) Chen, X.; Shen, S.; Guo, L.; Mao, S. S. Semiconductor-based photocatalytic hydrogen generation. *Chemical reviews* **2010**, *110*, 6503-6570.
(2) Karunadasa, H. I.; Montalvo, E.; Sun, Y.; Majda, M.; Long, J. R.; Chang, C. J. A molecular MoS_2 edge site mimic for catalytic hydrogen generation. *Science* **2012**, *335*, 698-702.
(3) Watanabe, M.; Inomata, H.; Arai, K. Catalytic hydrogen generation from biomass (glucose and cellulose) with ZrO_2 in supercritical water. *Biomass and Bioenergy* **2002**, *22*, 405-410.
(4) Yang, H. G.; Sun, C. H.; Qiao, S. Z.; Zou, J.; Liu, G.; Smith, S. C.; Cheng, H. M.; Lu, G. Q. Anatase TiO_2 single crystals with a large percentage of reactive facets. *Nature* **2008**, *453*, 638.
(5) Cornu, C. J.; Colussi, A.; Hoffmann, M. R. Quantum yields of the photocatalytic oxidation of formate in aqueous TiO2 suspensions under continuous and periodic illumination. *The Journal of Physical Chemistry B* **2001**, *105*, 1351-1354.
(6) Mrowetz, M.; Selli, E. H_2O_2 evolution during the photocatalytic degradation of organic molecules on fluorinated TiO_2. *New Journal of Chemistry* **2006**, *30*, 108-114.
(7) Montoya, J.; Velasquez, J.; Salvador, P. The direct–indirect kinetic model in photocatalysis: a reanalysis of phenol and formic acid degradation rate dependence on photon flow and concentration in TiO_2 aqueous dispersions. *Applied Catalysis B: Environmental* **2009**, *88*, 50-58.
(8) Ide, Y.; Inami, N.; Hattori, H.; Saito, K.; Sohmiya, M.; Tsunoji, N.; Komaguchi, K.; Sano, T.; Bando, Y.; Golberg, D. Remarkable charge separation and photocatalytic efficiency enhancement through interconnection of TiO_2 nanoparticles by hydrothermal treatment. *Angewandte Chemie International Edition* **2016**, *55*, 3600-3605.
(9) Feng, C.; Hao, Y.; Zhang, L.; Shang, N.; Gao, S.; Wang, Z.; Wang, C. AgPd nanoparticles supported on zeolitic imidazolate framework derived N-doped porous carbon as an efficient catalyst for formic acid dehydrogenation. *RSC Advances* **2015**, *5*, 39878-39883.
(10) Alamgholiloo, H.; Zhang, S.; Ahadi, A.; Rostamnia, S.; Banaei, R.; Li, Z.; Liu, X.; Shokouhimehr, M. Synthesis of bimetallic 4-PySI-Pd@ Cu (BDC) via open metal site Cu-MOF: Effect of metal and support of Pd@ Cu-MOFs in H2 generation from formic acid. *Molecular Catalysis* **2019**, *467*, 30-37.

(11) Ha, S.; Larsen, R.; Masel, R. Performance characterization of Pd/C nanocatalyst for direct formic acid fuel cells. *Journal of Power Sources* **2005**, *144*, 28-34.
(12) Larsen, R.; Ha, S.; Zakzeski, J.; Masel, R. I. Unusually active palladium-based catalysts for the electrooxidation of formic acid. *Journal of Power Sources* **2006**, *157*, 78-84.
(13) Blasco, T.; Corma, A.; Navarro, M.; Pariente, J. P. Synthesis, characterization, and catalytic activity of Ti-MCM-41 structures. *Journal of Catalysis* **1995**, *156*, 65-74.
(14) Zhang, W.; Fröba, M.; Wang, J.; Tanev, P. T.; Wong, J.; Pinnavaia, T. J. Mesoporous titanosilicate molecular sieves prepared at ambient temperature by electrostatic ($S^+ I^-$, $S^+ X^-I^+$) and neutral (S° I°) assembly pathways: a comparison of physical properties and catalytic activity for peroxide oxidations. *Journal of the American Chemical Society* **1996**, *118*, 9164-9171.
(15) Corma, A.; Camblor, M.; Esteve, P.; Martinez, A.; Perezpariente, J. Activity of Ti-Beta catalyst for the selective oxidation of alkenes and alkanes. *Journal of Catalysis* **1994**, *145*, 151-158.
(16) Koyano, K. A.; Tatsumi, T. Synthesis of titanium-containing mesoporous molecular sieves with a cubic structure. *Chemical communications* **1996**, 145-146.
(17) Morey, M. S.; O'Brien, S.; Schwarz, S.; Stucky, G. D. Hydrothermal and postsynthesis surface modification of cubic, MCM-48, and ultralarge pore SBA-15 mesoporous silica with titanium. *Chemistry of materials* **2000**, *12*, 898-911.
(18) Bagshaw, S. A.; Prouzet, E.; Pinnavaia, T. J. Templating of mesoporous molecular sieves by nonionic polyethylene oxide surfactants. *Science* **1995**, *269*, 1242-1244.
(19) Bagshaw, S. A.; Di Renzo, F.; Fajula, F. Preparation of metal-incorporated MSU mesoporous silica molecular sieves. Ti incorporation via a totally non-ionic route. *Chemical Communications* **1996**, 2209-2210.
(20) Ungureanu, A.; On, D. T.; Dumitriu, E.; Kaliaguine, S. Hydroxylation of 1-naphthol by hydrogen peroxide over UL-TS-1 and TS-1 coated MCF. *Applied Catalysis A: General* **2003**, *254*, 203-223.
(21) Chen, Y.; Huang, Y.; Xiu, J.; Han, X.; Bao, X. Direct synthesis, characterization and catalytic activity of titanium-substituted SBA-15 mesoporous molecular sieves. *Applied Catalysis A: General* **2004**, *273*, 185-191.
(22) Wu, S.; Han, Y.; Zou, Y.-C.; Song, J.-W.; Zhao, L.; Di, Y.; Liu, S.-Z.; Xiao, F.-S. Synthesis of heteroatom substituted SBA-15 by the "pH-adjusting" method. *Chemistry of materials* **2004**, *16*, 486-492.
(23) Bérubé, F.; Kleitz, F.; Kaliaguine, S. A comprehensive study of titanium-substituted SBA-15 mesoporous materials prepared by direct synthesis. *The Journal of Physical Chemistry C* **2008**, *112*, 14403-14411.
(24) Bérubé, F.; Kleitz, F.; Kaliaguine, S. Surface properties and epoxidation catalytic activity of Ti-SBA15 prepared by direct synthesis. *Journal of materials science* **2009**, *44*, 6727.
(25) Gong, Y.; Wang, D. P.; Wu, R.; Gazi, S.; Soo, H. S.; Sritharan, T.; Chen, Z. New insights into the photocatalytic activity of 3-D core–shell P25@ silica nanocomposites: impact of mesoporous coating. *Dalton Transactions* **2017**, *46*, 4994-5002.
(26) Abedi, S.; Karimi, B.; Kazemi, F.; Bostina, M.; Vali, H. Amorphous TiO 2 coated into periodic mesoporous organosilicate channels as a new binary photocatalyst for regeneration of carbonyl compounds from oximes under sunlight irradiation. *Organic & biomolecular chemistry* **2013**, *11*, 416-419.
(27) Yang, J.; Zhang, J.; Zhu, L.; Chen, S.; Zhang, Y.; Tang, Y.; Zhu, Y.; Li, Y. Synthesis of nano titania particles embedded in mesoporous SBA-15: characterization and photocatalytic activity. *Journal of Hazardous Materials* **2006**, *137*, 952-958.

(28) Busuioc, A. M.; Meynen, V.; Beyers, E.; Mertens, M.; Cool, P.; Bilba, N.; Vansant, E. F. Structural features and photocatalytic behaviour of titania deposited within the pores of SBA-15. *Applied Catalysis A: General* **2006**, *312*, 153-164.
(29) Abedi, S.; Morsali, A. Ordered mesoporous metal–organic frameworks incorporated with amorphous TiO2 as photocatalyst for selective aerobic oxidation in sunlight irradiation. *ACS Catalysis* **2014**, *4*, 1398-1403.
(30) Van Der Voort, P.; Esquivel, D.; De Canck, E.; Goethals, F.; Van Driessche, I.; Romero-Salguero, F. J. Periodic mesoporous organosilicas: from simple to complex bridges; a comprehensive overview of functions, morphologies and applications. *Chemical Society Reviews* **2013**, *42*, 3913-3955.
(31) Muth, O.; Schellbach, C.; Fröba, M. Triblock copolymer assisted synthesis of periodic mesoporous organosilicas (PMOs) with large poresElectronic f. *Chemical Communications* **2001**, 2032-2033.
(32) Li, Y.-J.; Wang, L.; Yan, B. Photoactive lanthanide hybrids covalently bonded to functionalized periodic mesoporous organosilica (PMO) by calix [4] arene derivative. *Journal of Materials Chemistry* **2011**, *21*, 1130-1138.
(33) Doustkhah, E.; Rostamnia, S.; Imura, M.; Ide, Y.; Mohammadi, S.; Hyland, C. J.; You, J.; Tsunoji, N.; Zeynizadeh, B.; Yamauchi, Y. Thiourea bridged periodic mesoporous organosilica with ultra-small Pd nanoparticles for coupling reactions. *RSC Advances* **2017**, *7*, 56306-56310.
(34) Rostamnia, S.; Doustkhah, E.; Bulgar, R.; Zeynizadeh, B. Supported palladium ions inside periodic mesoporous organosilica with ionic liquid framework (Pd@ IL-PMO) as an efficient green catalyst for S-arylation coupling. *Microporous and Mesoporous Materials* **2016**, *225*, 272-279.
(35) Doustkhah, E.; Rostamnia, S.; Zeynizadeh, B.; Kim, J.; Yamauchi, Y.; Ide, Y. Efficient H2 Generation Using Thiourea-based Periodic Mesoporous Organosilica with Pd Nanoparticles. *Chemistry Letters* **2018**, *47*, 1243-1245.
(36) Ahadi, A.; Rostamnia, S.; Panahi, P.; Wilson, L. D.; Kong, Q.; An, Z.; Shokouhimehr, M. Palladium Comprising Dicationic Bipyridinium Supported Periodic Mesoporous Organosilica (PMO): Pd@ Bipy–PMO as an Efficient Hybrid Catalyst for Suzuki–Miyaura Cross-Coupling Reaction in Water. *Catalysts* **2019**, *9*, 140.
(37) Bashti, A.; Kiasat, A. R.; Mokhtari, B. Synthesis and characterization of dicationic 4, 4′-bipyridinium dichloride ordered mesoporous silica nanocomposite and its application in the preparation of 1 H-pyrazolo [1, 2-b] phthalazine-5, 10-dione derivatives. *RSC Advances* **2015**, *5*, 25816-25823.
(38) Ng, L. K.-S.; Tan, E. J.-C.; Goh, T. W.; Zhao, X.; Chen, Z.; Sum, T. C.; Soo, H. S. Mesoporous SiO_2/$BiVO_4$/CuOx nanospheres for Z-scheme, visible light aerobic C–N coupling and dehydrogenation. *Applied Materials Today* **2019**, *15*, 192-202.
(39) Halasi, G.; Schubert, G. b.; Solymosi, F. Photodecomposition of formic acid on N-doped and metal-promoted TiO_2 production of CO-free H_2. *The Journal of Physical Chemistry C* **2012**, *116*, 15396-15405.
(40) Miller, K. L.; Lee, C. W.; Falconer, J. L.; Medlin, J. W. Effect of water on formic acid photocatalytic decomposition on TiO2 and Pt/TiO_2. *Journal of Catalysis* **2010**, *275*, 294-299.
(41) Liao, L.-F.; Wu, W.-C.; Chen, C.-Y.; Lin, J.-L. Photooxidation of formic acid vs formate and ethanol vs ethoxy on TiO_2 and effect of adsorbed water on the rates of formate and formic acid photooxidation. *The Journal of Physical Chemistry B* **2001**, *105*, 7678-7685.

(42)Honda, Y.; Watanabe, M.; Hagiwara, H.; Ida, S.; Ishihara, T. Inorganic/whole-cell biohybrid photocatalyst for highly efficient hydrogen production from water. *Applied Catalysis B: Environmental* **2017**, *210*, 400-406.

(43) Cao, L.; Wang, Y. Photocatalysis of viologens for photoinitiated polymerization using carboxylic acid as electron donors. *Journal of photochemistry and photobiology A: Chemistry* **2017**, *333*, 63-69.